

# Control of dynamical localization by an additional quantum degree of freedom

K. Riedel, P. Törmä, V. Savichev, and W. P. Schleich

*Abteilung für Quantenphysik, Universität Ulm, D-89069 Ulm, Germany*

(August 7, 2018)

We identify a new parameter that controls the localization length in a driven quantum system. This parameter results from an additional quantum degree of freedom. The center-of-mass motion of a two-level ion stored in a Paul trap and interacting with a standing wave laser field exhibits this phenomenon. We also discuss the influence of spontaneous emission.

PACS numbers: 42.50.-p, 05.45.+b, 03.65.Sq

## I. INTRODUCTION

The phenomenon of localization manifests itself in many quantum mechanical systems ranging from the localization of light in a random medium [1], to Anderson localization of an electronic wave [2] and to atoms in time-dependent laser fields [3,4]. In all these cases the underlying classical system is chaotic and shows diffusion as a function of time. In contrast, the quantum mechanical counterpart has a localized wave function whose width is governed by the classical diffusion and Planck's constant [5,6]. In the present paper we show that there exists an additional quantum parameter that controls the localization length. In the system of a two-level ion stored in a Paul trap [7] and interacting with a standing wave it is the detuning between the transition frequency of the ion and the laser frequency.

A recent paper [8] has shown that a stored ion moving along a far-detuned standing wave shows localization in position and momentum variables. In this work we have neglected the internal structure of the ion. We have therefore only considered the quantum dynamics of a particle moving in a one-dimensional time-dependent potential. In the present paper we extend this analysis and consider the motion of an ion taking into account its internal dynamics.

Our paper is organized as follows: In Sec. II we first summarize the essential ingredients of the problem. In particular, we introduce the relevant equations and describe the methods of solution for the classical and quantum mechanical equations of motion. We also define the quantities which we calculate such as the position and momentum distributions and their moments.

In Sec. III we discuss the dependence of the classical and quantum mechanical position and momentum distributions on the detuning. We find characteristic oscillations in the widths of these distributions as a function of the detuning. These oscillations are absent in the corre-

sponding classical curves. We explain these structures by transforming the Hamiltonian into an interaction picture.

We emphasize that this is different to the case of atoms moving in a phase modulated standing wave. There the corresponding oscillations appear in the widths of the quantum as well as of the classical momentum distributions [9–11]. Hence, the detuning is an additional parameter controlling the width and the shape of the quantum distributions.

Moreover, in the quantum systems discussed so far in the context of dynamical localization the quantum diffusion is always slower than the classical one. However, in the present model the new control parameter detuning can create situations in which the quantum diffusion temporarily exceeds the classical one.

Quantum interference effects such as dynamical localization are extremely sensitive to decoherence arising for example from noise or spontaneous emission [12]. We are therefore forced to investigate in Sec. IV the influence of spontaneous emission. We find that the drastic difference between quantum and classical behavior is preserved in the limit of a far off-resonance situation. We conclude in Sec. V by summarizing our main results.

## II. FORMULATION OF THE PROBLEM

We consider the standard Paul trap set-up realized experimentally in many labs [13–15]: a standing electromagnetic wave of frequency  $\omega_L$  and wave number  $k$  aligned along the  $x$ -axis couples the internal states  $|g\rangle$  and  $|e\rangle$  of a single two-level ion of mass  $m$  to the center-of-mass motion. The resulting dynamics of the ion follows from the time-dependent Schrödinger equation with the Hamiltonian

$$\hat{H} = \frac{\hat{p}^2}{2m} + \frac{1}{2} \frac{m\omega^2}{4} [a + 2q \cos(\omega\tilde{t})] \hat{x}^2 + \frac{1}{2} \hbar\omega_0 \hat{\sigma}_z + \hbar\hat{\Omega}_0 \hat{\sigma}_x \cos(k\hat{x}) \cos(\omega_L \tilde{t}). \quad (1)$$

Here the parameters  $a$  and  $q$  are proportional [7] to the DC and AC voltages applied to the trap and  $\sigma_x, \sigma_z$  are the standard Pauli matrices. Moreover, we denote the frequencies of the AC field, the atomic transition, the Rabi frequency by  $\omega, \omega_0$ , and  $\hat{\Omega}_0$ , respectively.

We introduce the dimensionless position  $\hat{x} \equiv k\hat{x}$ , time  $t \equiv \omega\tilde{t}/2$  and momentum  $\hat{p} \equiv \frac{2k}{m\omega}\hat{p}$ . When we transform into an interaction picture with the unitary transformation  $\exp(i\omega_L \sigma_z t/2)$  the dimensionless Hamiltonian in rotating wave approximation reads

$$\hat{H} \equiv \frac{4k^2}{m\omega^2} \hat{H} = \frac{1}{2} \hat{p}^2 + \frac{1}{2} [a + 2q \cos(2t)] \hat{x}^2 - \kappa \Delta \hat{\sigma}_z + \kappa \Omega_0 \hat{\sigma}_x \cos \hat{x}. \quad (2)$$

Here we have defined the dimensionless Rabi frequency  $\Omega_0 \equiv \tilde{\Omega}_0/\omega$  and detuning  $\Delta = (\omega_L - \omega_0)/\omega$ .

The dynamics of the ion follows from the time-dependent Schrödinger equation

$$i\kappa \frac{\partial |\Psi(t)\rangle}{\partial t} = \hat{H} |\Psi(t)\rangle \quad (3)$$

for the state vector

$$|\Psi(t)\rangle = \int dx [\Psi_g(x, t)|g\rangle + \Psi_e(x, t)|e\rangle] |x\rangle. \quad (4)$$

Here the effective Planck constant  $\kappa \equiv 2k^2\hbar/(m\omega)$  is consistent with the commutation relation  $[\hat{x}, \hat{p}] = 2k^2/(m\omega)[\hat{x}, \hat{p}] = 2k^2/(m\omega)i\hbar \equiv i\kappa$ .

The state vector  $|\Psi\rangle$  provides the probabilities

$$P_g(x, t) \equiv |\Psi_g(x, t)|^2 \quad (5)$$

or

$$P_e(x, t) \equiv |\Psi_e(x, t)|^2 \quad (6)$$

to find the ion at the time  $t$  at position  $x$  given it is in the internal state  $|g\rangle$  or  $|e\rangle$ , respectively. When we are not interested in the internal states the position probability distribution  $P(x, t)$  reads

$$P(x, t) \equiv |\Psi_g(x, t)|^2 + |\Psi_e(x, t)|^2. \quad (7)$$

We simulate the effect of spontaneous emission by the quantum Monte-Carlo method [16,17] using the effective non-hermitian Hamiltonian

$$\hat{H}_{\text{eff}} \equiv \hat{H} - i\kappa \frac{\gamma}{2} \hat{\sigma}_+ \hat{\sigma}_-.$$

Here we introduced the atomic operators  $\sigma_+ \equiv |e\rangle\langle g|$  and  $\sigma_- \equiv |g\rangle\langle e|$ , and  $\gamma$  is the spontaneous decay rate scaled by  $\omega$ .

The moments of time when a spontaneous emission event takes place are chosen at random. Then the wave function is projected onto the ground state and renormalized, that is  $|\Psi\rangle \rightarrow \hat{\sigma}_- |\Psi\rangle / \langle \Psi | \hat{\sigma}_- | \Psi \rangle$ . The recoil  $p \in [-\kappa, \kappa]$  is chosen randomly according to the probability distribution [18]

$$N(p) \equiv \frac{3}{8\kappa} \left( 1 + \left( \frac{p}{\kappa} \right)^2 \right),$$

of dipole radiation. When the results of single runs are averaged, we obtain the same result as predicted by a master equation [16,17].

As an initial condition for the internal states we use the superposition  $(|g\rangle + |e\rangle)/\sqrt{2}$  and the center-of-mass wave function is a Gaussian of width  $\Delta x = \sqrt{\kappa}$ . In

order to investigate localization we start with this wave packet at the origin where the classical phase space is a stochastic sea [8,19]. We calculate the time evolution using the split-operator method [20] with a grid of 8192 points. We control numerical errors using an adaptive time step-size algorithm [21].

This numerical integration allows us to find the time dependence of the position probability distributions  $P_g(x, t)$ ,  $P_e(x, t)$  and  $P(x, t)$ . Moreover, we calculate the corresponding momentum distributions where the wave functions  $\Psi_g$  and  $\Psi_e$  in position space are replaced by the wave functions in momentum space.

We compare and contrast these quantum results to the dynamics [22] resulting from the classical equations of motion [19,23]

$$\begin{aligned} \dot{x} &= p \\ \dot{p} &= -(a + 2q \cos(2t))x + \kappa \Omega_0 \sin(x)r_1 \end{aligned} \quad (8)$$

for the center-of-mass motion. These equations are driven by the Bloch equations [24]

$$\begin{aligned} \dot{r}_1 &= -2\Delta r_2 \\ \dot{r}_2 &= 2\Delta r_1 + 2\Omega_0 \cos(x)r_3 \\ \dot{r}_3 &= -2\Omega_0 \cos(x)r_2 \end{aligned} \quad (9)$$

describing the internal dynamics. Here  $r_1$ ,  $r_2$ , and  $r_3$  denote the in- and out-of-phase quadratures of the dipole moment, and the atomic inversion, respectively.

For the comparison with the quantum mechanical results we calculate 4096 trajectories starting from a classical Gaussian ensemble centered initially at the origin and having the same widths in position and momentum as the quantum wave packet. In this way we obtain the classical phase space distribution from which we find by integration over  $x$  or  $p$  the classical momentum or position distributions  $P_{cl}(p)$  or  $P_{cl}(x)$ .

### III. INFLUENCE OF THE DETUNING

In the present section we study the influence of the detuning of the laser field with respect to the atomic transition on the dynamics of the system. Here we consider the following quantities of interest: the classical and quantum distributions, and their width as a function of time and detuning.

In Fig. 1 we show the influence of the internal structure of the ion on the classical and on the quantum diffusion. Here we analyze for various detunings  $\Delta$  the time dependence of the widths  $\Delta x$  (left column) of the classical (thin lines) and quantum mechanical (thick lines) position distributions  $P_{cl}(x, t)$  and  $P(x, t)$  (right column). Whereas the left column emphasizes the time dependence of the widths, the right column shows position distributions averaged over the time interval  $[450\pi, 500\pi]$ . In order to bring out most clearly the influence of the detuning we have neglected spontaneous emission in this figure.

For a very small detuning the quantum width  $\Delta x$  lies well below the classical one. The latter increases as a function of time. In contrast, the quantum result displays oscillations around a steady-state value. This suppression of the classical diffusion is due to dynamical localization as discussed in Ref. [8].

However, for slightly larger detunings the quantum curve is still oscillating but reaches partially above the classical one. For even larger detunings the quantum curve falls again below the classical one. Eventually for larger detunings it again goes partially above. Hence, for a fixed detuning, there exist time regimes in which the quantum diffusion is stronger than the classical one.

This detuning dependence of the quantum diffusion manifests itself in the shape of the quantum mechanical position distribution. The latter consists of a sharp peak and a broad background. The detuning essentially controls the shape of the background: Depending on  $\Delta$  we find distributions either of negative or positive curvature. In contrast, the detuning hardly influences the classical distributions shown on the right column by thin curves. We emphasize that the momentum distributions not shown here display almost identical behavior.

To discuss the influence of the detuning on the localization length we show in Fig. 2 the widths  $\Delta x$  of the classical and the quantum distributions averaged from  $t = 200\pi$  to  $500\pi$ . We note characteristic oscillations in the quantum mechanical curve as a function of the detuning  $\Delta$ . These oscillations do not appear in the classical curve which decreases monotonously for increasing  $\Delta$ . This feature becomes clear when we recall that the width of the classical distribution at a given time is determined by the classical diffusion constant. The latter is proportional to the perturbing potential caused by the laser field. In the limiting case of large detuning, the effective potential becomes [25] proportional to the effective coupling constant  $\Omega_0^2/\Delta$ . As  $\Delta$  increases, the perturbation decreases and hence the diffusion is slower.

An interesting domain is a small region around  $\Delta = 0$ . Here the classical diffusion rate sharply decreases. The explanation of this feature follows from the set of Eqs. (8) and (9): The effective potential provided by the laser field in Eq. (8) is proportional to the factor  $r_1(t)$ . This quantity can take the maximum value of unity. For the resonant case,  $\Delta = 0$ , we have  $\dot{r}_1 = 0$  and hence  $r_1$  is independent of time and determined by the initial condition. The Bloch vector coordinates corresponding to the initial state  $(|g\rangle + |e\rangle)/\sqrt{2}$  are  $r_1(0) = 1, r_2(0) = 0$  and  $r_3(0) = 0$ . Hence  $r_1 = 1$  results in the maximum driving strength of the center-of-mass motion.

The curve for the quantum widths shows a distinctly different behaviour with a lot of structure. In particular, for  $\Delta < 1$  we note a well-developed resonance structure and two sharp minima and maxima. The minimum around  $\Delta = 0$  is related to the separable quantum dynamics in the two diabatic potentials  $V^{(\pm)} = \frac{1}{2}[a + 2q \cos(2t)]x^2 \pm \hbar\Omega_0 \cos x$ .

To bring this out most clearly we transform from the

$|g\rangle, |e\rangle$  basis states to their superpositions  $|+\rangle \equiv (|g\rangle + |e\rangle)/\sqrt{2}$ , and  $|-\rangle \equiv (|g\rangle - |e\rangle)/\sqrt{2}$ . In this basis the Hamiltonian Eq. (2) reads

$$\hat{H} = \frac{1}{2}\hat{p}^2 + \frac{1}{2}[a + 2q \cos(2t)]\hat{x}^2 + \hbar\Omega_0\hat{\sigma}_z \cos \hat{x} + \hbar\Delta\hat{\sigma}_x, \quad (10)$$

and the coupling is now proportional to the detuning  $\Delta$ . Hence we indeed find the potentials  $V^{(\pm)}$ .

When we now increase the detuning, transitions between the states  $|+\rangle$  and  $|-\rangle$  contribute to the quantum diffusion. Therefore, the quantum diffusion rate quickly rises to the maximal classical one; this corresponds to the formation of the first maximum.

The next minimum fits the condition  $\Delta \approx \omega_s$ , where  $\omega_s = 0.29$  is the secular frequency of the trap. The origin of this resonance becomes clear, when we write the Hamiltonian, Eq. (2), in the interaction picture where the dynamics of the trap as well as the internal state energy are transformed away by unitary transformations [26]. In this picture the Hamiltonian reads

$$H_{\text{int}}(t) = \sum_{n=0}^{\infty} \sum_{k=-[n/2]}^{\infty} \sum_{l=-\infty}^{\infty} \hbar\omega_l^{(n,n+2k)} e^{2i(l-k\omega_s+\Delta)t} \times \sigma_+ |n\rangle \langle n+2k| + \text{h.c.} \quad (11)$$

with the Lamb-Dicke parameter  $\eta \equiv [\hbar/(2\omega_r)]^{1/2}$  and

$$\omega_l^{(n,n+2k)} \equiv \Omega_0 \sqrt{\frac{n!}{(n+2k)!}} [i\eta]^{2k} \frac{1}{\pi} \times \int_{-\pi/2}^{\pi/2} dt [\phi^*(t)]^{2k} e^{-\frac{1}{2}\eta^2|\phi(t)|^2} L_n^{2k}(\eta^2|\phi(t)|^2) e^{-2ilt}. \quad (12)$$

Here  $|n\rangle$  denotes the  $n$ -th energy eigenstate of the time independent reference oscillator [27] with frequency  $\omega_r$ . Moreover, we have made use of the Floquet solution  $\epsilon(t) = \exp(i\omega_s t)\phi(t)$ , where  $\phi(t) = \phi(t + \pi)$  is a periodic function. The solution  $\epsilon(t)$  obeys [27] the differential equation

$$\ddot{\epsilon} + [a + 2q \cos(2t)]\epsilon = 0 \quad (13)$$

with  $\epsilon(0) = 1$  and  $\dot{\epsilon}(0) = i\omega_r$ .

From the term  $e^{2i(l-k\omega_s+\Delta)t}$  in the Hamiltonian (11) we expect resonance effects, when  $\Delta$  satisfies the condition  $l - k\omega_s + \Delta = 0$ . For  $l = 0, k = 1$  we have  $\Delta = \omega_s$ , which corresponds to two-phonon transitions. This resonance suggests an enhancement of the quantum diffusion rate on resonance. Instead, we have a deep minimum.

In order to understand this counter-intuitive behavior we calculate the characteristic frequencies  $\omega_l^{(n,n+2k)}$  for  $l = 0$  and  $k = 1, 2$  at different vibrational quantum numbers  $n$ . From the inset of Fig. 2 we recognize that  $|\omega_0^{(n,n+2)}|$  has a deep minimum around  $n = 10$ , which explains suppression of the diffusion over the vibrational

states. As shown by the curve in the inset for  $|\omega_0^{(n,n+4)}|$  there is no minimum just a decay. This causes the quantum diffusion to take on the classical value, which explains the formation of the second maximum [28].

We conclude this section by noting that the phenomenon of oscillations in the width of distributions also appears in another quantum system showing classical chaos and quantum localization: an atom moving in a phase-modulated standing wave [9,10]. However in this case the oscillations are of classical origin and appear both in the classical and quantum widths.

#### IV. INFLUENCE OF SPONTANEOUS EMISSION

We now consider the effect of spontaneous emission using the quantum Monte-Carlo technique [16,17]. The purpose of our investigations is twofold. First, we want to show that indeed the phenomena discussed so far are quantum interference effects. They are therefore sensitive to decoherence such as spontaneous emission. The latter predominantly occurs when the laser is tuned close to resonance with the atomic transition. Second, we want to show that in the far-detuned limit the effect of decoherence is negligible and the phenomenon of dynamical localization survives.

In Fig. 3 we show the results of our simulations with a realistic rate of spontaneous emission corresponding to the decay rate of the  $S \rightarrow P$  transition at 19.4 MHz in  ${}^9\text{Be}^+$  [29]. We compare them to the classical and to the quantum result without noise. The loss of the coherence causes destruction of localization. In this case the widths of the quantum mechanical position and momentum distributions are larger than the classical ones. This additional diffusion is caused by the random recoil kicks following each spontaneous emission event. When we neglect the recoil — which of course is not realistic — the quantum curve follows the classical one. The position and momentum distributions are of classical type, that is on the logarithmic scale they are polynomial curves. Note that the pattern of the standing wave appears on top of the position distributions.

In Fig. 4 we show the results for  $\Delta = 1000$ , corresponding to a detuning of 10 GHz, a value which was mentioned in Ref. [8]. The small oscillations in the quantum widths  $\Delta x$  and  $\Delta p$  are destroyed, but the main phenomenon, the substantial quantum suppression of classical diffusion is still visible.

It is interesting to note that in a single realization of the dynamics the coherence of the two-level superposition is completely destroyed by a single spontaneous emission. However, it affects only slightly the motional coherence because the population of the excited state is very low. Furthermore, the small difference between the results with and without spontaneous emission in Fig. 4 is of the same order of magnitude that was found for the problem of an atom in a phase modulated standing wave

[30].

In the position distribution of the ground state, there is more probability in the classical-like background than in the case of no spontaneous emission. We have found that this background is very slowly growing, and no real steady state can be reached. However, if we increase the detuning, the real steady state is approached asymptotically. Since dynamical localization appears for a large range of parameters [8], there is a lot of room for optimizing the parameters. Thus the phenomenon of dynamical localization in a Paul trap could be observed experimentally.

In order to observe not only dynamical localization but also the oscillations in the localization length discussed in the previous section, one should consider a configuration where decoherence is weaker even for small detunings, for example a different set of parameters in the present system, or a different system such as a Raman transition between two ground states.

#### V. CONCLUSIONS

There are basically two ways of controlling dynamical localization: (i) through the classical diffusion and (ii) through the quantized nature of the variable showing localization. This stands out most clearly in the estimate  $l \sim D/\hbar^2$  for the localization length. Here  $D$  is the classical diffusion coefficient determined by the perturbing potential. The coupling to this potential is called the control parameter, since it is a direct way to control the localization length. The scaled Planck constant  $\hbar$  describes how important the quantization of the system is with respect to the perturbation.

In this paper we have shown that, when the perturbing potential has a quantum character as well, the relation  $l \sim D/\hbar^2$  is not exactly true anymore; we observe oscillations in the localization length which do not appear in the classical diffusion rate. The parameter determining the oscillations could be called the quantum control parameter.

#### ACKNOWLEDGMENTS

We thank B. Kneer and M. El Ghafar for many fruitful discussions. P. T. and V. S. acknowledge the support of the Deutsche Forschungsgemeinschaft. We thank the Rechenzentrum Ulm and the Rechenzentrum Karlsruhe for their technical support.

---

[1] A. Legendijk and B. A. van Tiggelen, Phys. Rep. **270**, 143 (1996).

- [2] P. W. Anderson, *Phys. Rev.* **109**, 1492 (1958).
- [3] For a review see, for example P. M. Koch and K. A. H. van Leeuwen, *Phys. Rep.* **255**, 289 (1995); G. Casati, *Phys. Rev. A* **45**, 7670 (1992).
- [4] F. L. Moore, J. C. Robinson, C. Bharucha, P. E. Williams, and M. G. Raizen, *Phys. Rev. Lett.* **73**, 2974 (1994); theoretical proposal in R. Graham, M. Schlautmann, and P. Zoller, *Phys. Rev. A* **45**, R19 (1992).
- [5] F. Haake, *Quantum Signatures of Chaos* (Springer-Verlag, Berlin, 1992).
- [6] *Quantum Chaos*, Eds. G. Casati and B. Chirikov (Cambridge University Press, 1995).
- [7] W. Paul, *Rev. Mod. Phys.* **62**, 531 (1990).
- [8] M. El Ghafar, P. Törmä, V. Savichev, E. Mayr, A. Zeiler, and W. P. Schleich, *Phys. Rev. Lett.* **78**, 4181 (1997).
- [9] J. C. Robinson, C. Bharucha, F. L. Moore, R. Jahnke, G. A. Georgaki, M. G. Raizen, and B. Sundaram, *Phys. Rev. Lett.* **74**, 3963 (1995).
- [10] P. J. Bardroff, I. Bialynicki-Birula, D. S. Krähmer, G. Kurizki, E. Mayr, P. Stifter, and W. P. Schleich, *Phys. Rev. Lett.* **74**, 3959 (1995).
- [11] In the work of R. Graham and S. Miyazaki, *Phys. Rev. A* **53**, 2683 (1996) the problem of atoms in a phase modulated standing wave was considered without the adiabatic elimination of the upper state. However, the emphasis of that paper was on spontaneous emission, not on the effect of an additional quantum degree of freedom.
- [12] For experimental studies of the effect of noise and dissipation on dynamical localization see M. Arndt, A. Buchleitner, R. N. Mantegna, and H. Walther, *Phys. Rev. Lett.* **67**, 2435 (1991); F. L. Moore, J. C. Robinson, C. Bharucha, B. Sundaram, and M. G. Raizen, *Phys. Rev. Lett.* **75**, 4598 (1995); R. Blümel, A. Buchleitner, R. Graham, L. Sirko, U. Smilansky, and H. Walther, *Phys. Rev. A* **44**, 4521 (1991), H. Ammann, R. Gray, I. Shvarchuck, and N. Christensen, *Phys. Rev. Lett.* **80**, 4111 (1998); B. G. Klappauf, W. H. Oskay, D. A. Steck, and M. G. Raizen, *Phys. Rev. Lett.* **81**, 1203 (1998).
- [13] D. M. Meekhof, C. Monroe, B. E. King, W. M. Itano, and D. J. Wineland, *Phys. Rev. Lett.* **76**, 1796 (1996); C. Monroe, D. M. Meekhof, B. E. King, and D. J. Wineland, *Science* **272**, 1131 (1996); D. Leibfried, D. M. Meekhof, B. E. King, C. Monroe, W. M. Itano, and D. J. Wineland, *Phys. Rev. Lett.* **77**, 4281 (1996).
- [14] G. Birkel, J. A. Yeazell, R. Rückerl, and H. Walther, *Europhys. Lett.* **27**, 197 (1994); H. Katori, S. Schlipf, and H. Walther, *Phys. Rev. Lett.* **79**, 2221 (1997).
- [15] B. Appasamy, Y. Stalgies, and P. E. Toschek, *Phys. Rev. Lett.* **80**, 2805 (1998).
- [16] R. Dum, A. S. Parkins, P. Zoller, and C. W. Gardiner, *Phys. Rev. A* **46**, 4382 (1992); K. Mølmer, Y. Castin, and J. Dalibard, *J. Opt. Soc. Am. B* **10**, 524 (1993).
- [17] H. Carmichael, *An Open System Approach to Quantum Optics* (Springer-Verlag, Berlin, 1991)
- [18] J. Javanainen and S. Stenholm, *Appl. Phys.* **21**, 35 (1980).
- [19] For more information about the classical dynamics of this system see R. Chacón and J. I. Cirac, *Phys. Rev. A* **51**, 4900 (1994); M. El Ghafar, E. Mayr, V. Savichev, P. Törmä, A. Zeiler, and W. P. Schleich, *J. Mod. Opt.* **44**, 1985 (1997).
- [20] M. D. Feit, J. A. Fleck, and A. Steiger, *J. of Comput. Phys.* **47**, 412 (1982).
- [21] K. Riedel, *Quanteneffekte in Paul-Fallen, Dynamische Lokalisierung und Dekohärenz*, Diplomarbeit, Universität Ulm, 1997, unpublished.
- [22] G. M. Zaslavsky, *Chaos in Dynamic Systems* (Harwood Academic Publishers, Chur, 1985).
- [23] In deriving these equations, we have assumed that the quantum mechanical position distribution is very narrow and localized near the classical trajectory  $x(t)$ . This property allows us to take the slowly varying cosine potential out of the integrals.
- [24] L. Mandel and E. Wolf, *Optical Coherence and Quantum Optics* (Cambridge University Press, 1995)
- [25] A. P. Kazantsev, G. I. Surdutovich, and V. P. Yakovlev, *Mechanical Action of Light on Atoms* (World Scientific, Singapore, 1990).
- [26] P. J. Bardroff, C. Leichtle, G. Schrade, and W. P. Schleich, *Phys. Rev. Lett.* **77**, 2198 (1996); *ibid Acta Physica Slovaca* **46**, 231 (1996).
- [27] R. J. Glauber, *Laser Manipulation of Atoms and Ions*, Proc. Int. School of Physics 'Enrico Fermi' Course 118, edited by E. Arimondo, W. D. Phillips, and F. Strumia (North Holland, Amsterdam, 1992); see also G. Schrade, P. J. Bardroff, R. J. Glauber, C. Leichtle, V. Yakovlev, and W. P. Schleich, *Appl. Phys. B* **64**, 181 (1997).
- [28] There is a close similarity between such type behavior and the so-called Fano resonance: U. Fano, *Phys. Rev.* **124**, 1866 (1961).
- [29] S. R. Jefferts, C. Monroe, E. W. Bell, and D. J. Wineland, *Phys. Rev. A* **51**, 3112 (1995).
- [30] P. Goetsch and R. Graham, *Phys. Rev. A* **54**, 5345 (1996).

FIG. 1. Classical and quantum dynamics of the center-of-mass motion of a two-level ion stored in a Paul trap and interacting with a classical standing light wave. We show the influence of the detuning  $\Delta$  between the frequencies of the atomic transition and the light on the dynamics using probability distributions  $P(x)$  in position averaged over the time period  $[450\pi, 500\pi]$  (right column), and widths  $\Delta x \equiv [\langle x^2 \rangle - \langle x \rangle^2]^{1/2}$  (left column) as a function of time. For a very small detuning (top) the quantum mechanical width (thick line) lies below the classical width (thin line). Whereas the width of the classical position distribution increases monotonously as a function of time the corresponding quantum result displays oscillations around a steady-state value. This suppression of the diffusion is due to dynamical localization as discussed in Ref. [8]. For slightly larger detunings the quantum curve is still oscillating but goes above the classical one. For even larger detunings the quantum curve falls again below the classical one and the diffusion is suppressed by dynamical localization. However, for larger detunings (bottom) the quantum curve again starts to move across the classical one. We note that only the quantum curves show a strong dependence on the detuning. This dependence also manifests itself in the position distributions. Indeed  $\Delta$  influences the shapes of the quantum, but not of the classical distributions. Here and in Fig. 2 we do not account for spontaneous emission. We have used the scaled Rabi frequency  $\Omega_0 = 2.24$  of the standing wave and the trap parameters  $a = 0, q = 0.4$  corresponding to the secular frequency  $\omega_s = 0.29$ . The effective Planck constant is  $\hbar = 0.29$ .

FIG. 2. Dependence of the classical (dashed line) and quantum mechanical (solid line) variance  $\Delta x$  in position on the detuning  $\Delta$ . For each value of  $\Delta$  we have averaged the variances over the time window  $[200\pi, 500\pi]$ . Whereas the classical curve decays monotonously with a characteristic maximum on resonance, the quantum curve shows striking oscillations. The inset shows the amplitudes  $|\omega_0^{(n,n+2)}|$  and  $|\omega_0^{(n,n+4)}|$  determining the strengths of the 2-phonon and 4-phonon transitions in their dependences on the vibrational quantum number  $n$ . Whereas  $|\omega_0^{(n,n+2)}|$  has a minimum,  $|\omega_0^{(n,n+4)}|$  decays monotonously. This leads to a minimum or a maximum in  $\Delta x$  for  $\Delta = \omega_s$  or  $\Delta = 2\omega_s$ , respectively. The squares mark the values of  $\Delta x$  at the detunings used in Fig. 1. Here and in Fig. 3 the parameters are as in Fig. 1.

FIG. 3. Influence of spontaneous emission on dynamical localization for  $\Delta = 0$ , that is on atomic resonance: We show the time dependence of the widths  $\Delta x$  and  $\Delta p$  in position and momentum (left column) and the probability distributions  $P(x)$  and  $P(p)$  averaged over the time interval  $[200\pi, 250\pi]$  (right column). Fat, thin and thick curves indicate these quantities in the presence and absence of spontaneous emission and for the classical case, respectively. We note that spontaneous emission destroys localization and due to the recoil the quantum widths become even larger than the classical ones. In the absence of spontaneous emission the position distributions of the ground and excited state (jagged thin curve) are sharply peaked. Moreover they are identical due to the fact, that the initial internal state is the superposition  $(|e\rangle + |g\rangle)/\sqrt{2}$ . Spontaneous emission destroys the localization peak and enhances the population in the ground (upper fat curve) at the expense of the ions in the excited state (lower fat curve). In this case the quantum distributions in position and momentum are even broader than the corresponding classical ones (thick lines). The pattern of the standing wave reflects itself in the position distributions (upper right corner). It is more pronounced in the quantum mechanical curves than in the classical one. The results in the case of spontaneous emission have been obtained by averaging over a sufficient number of runs, in this case 79 runs. Here and in Fig. 4 the scaled rate of spontaneous emission is  $\gamma = 2$ .

FIG. 4. Influence of spontaneous emission on dynamical localization for  $\Delta = 1000$ , that is far off-resonance. As in Fig. 3 we show the widths in position and momentum as a function of time and the corresponding probability distributions averaged over the time interval  $[200\pi, 250\pi]$ . Since we start from the ground state of the ion the strong detuning prevents the population of the excited state. We therefore only display the ground state population (fat line). We emphasize that this curve differs only slightly from the corresponding curve in the absence of spontaneous emission (thin line). Spontaneous emission does not destroy the localization. Due to the small amount of spontaneous emission an average over 49 runs was sufficient. In order to make contact with Ref. [8] we used the parameters  $\Omega_0 = 94.69$  and  $\hbar = 0.0725$ .

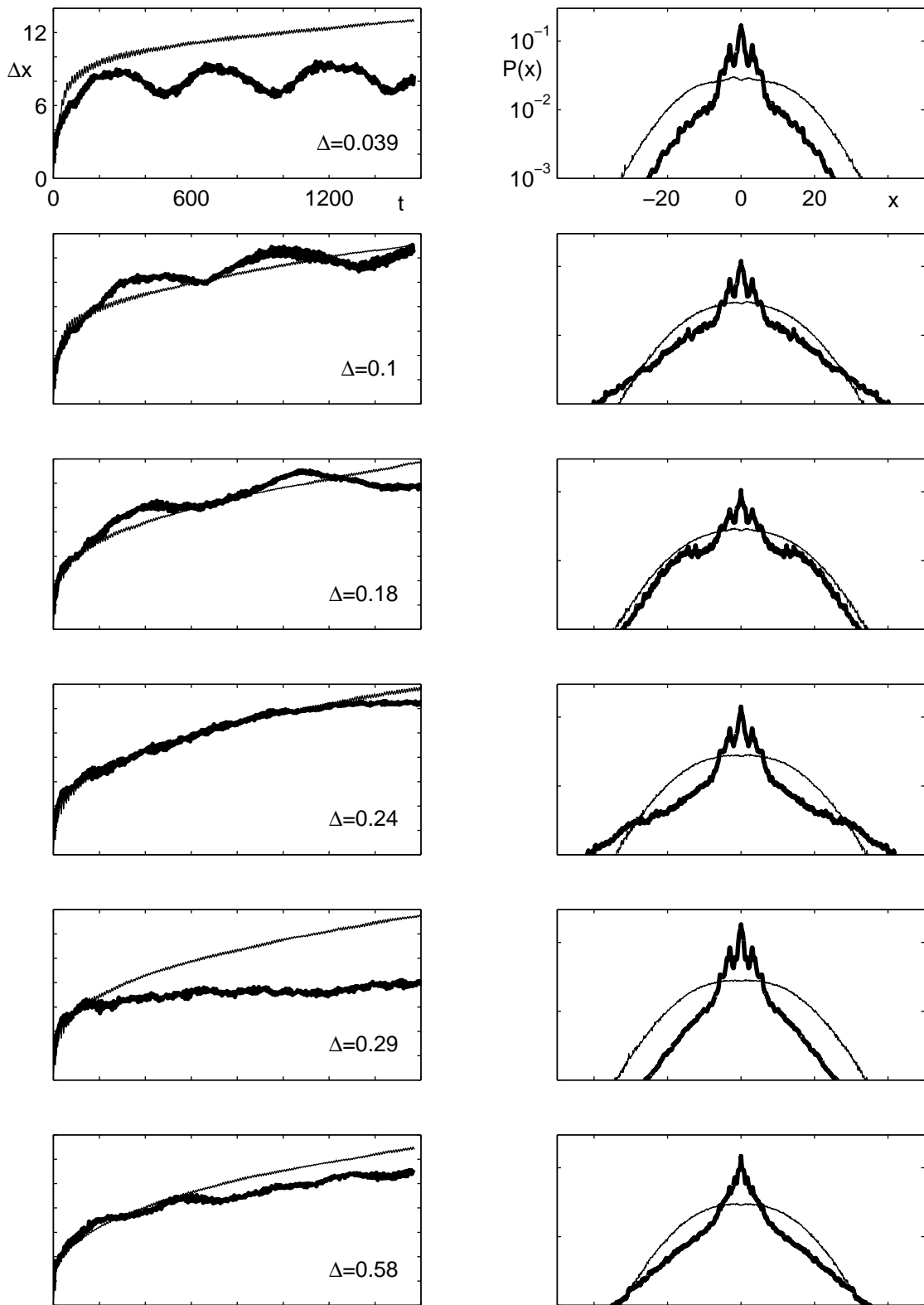


Fig.1, Riedel et al., PRA

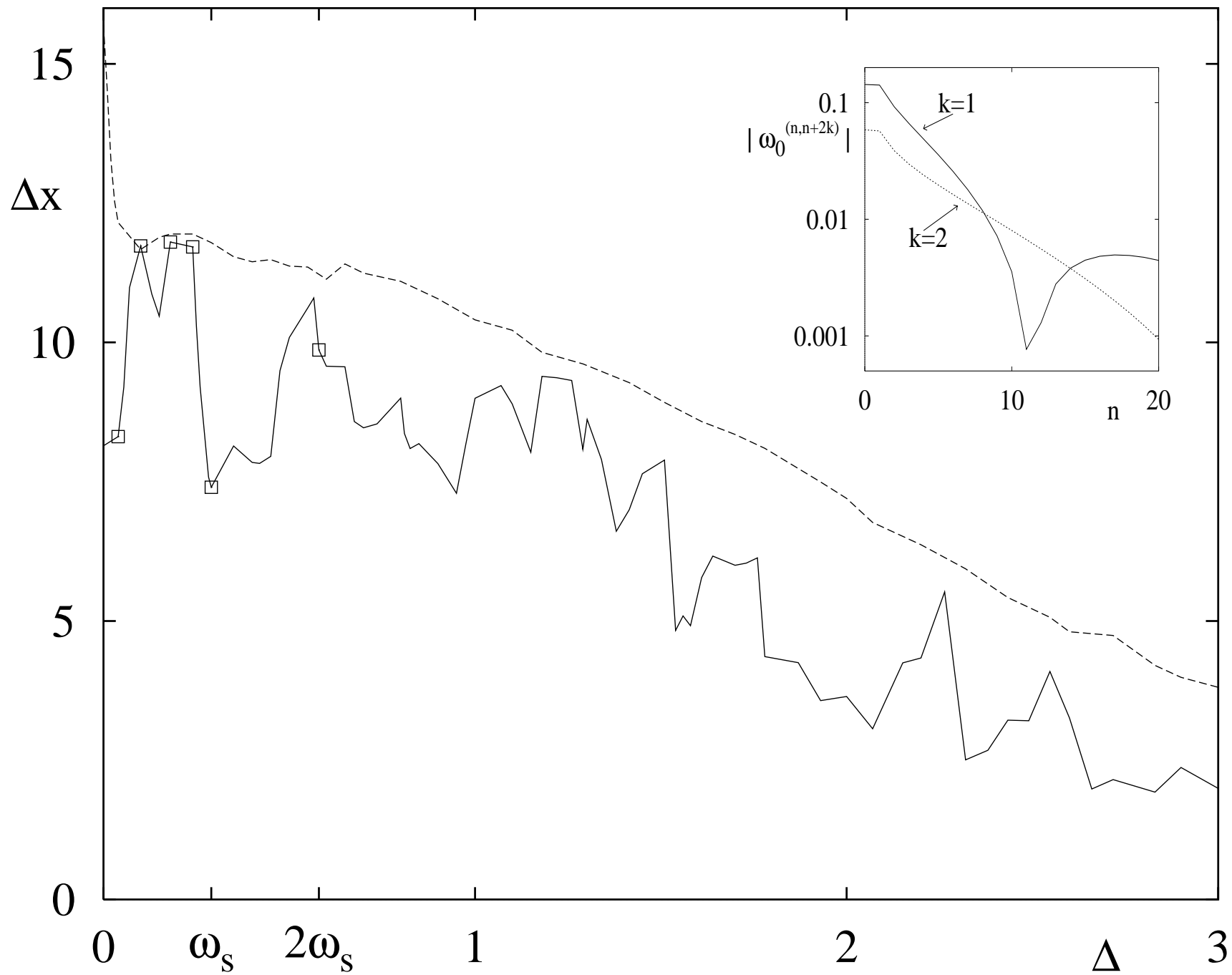


Fig. 2, Riedel et al., PRA



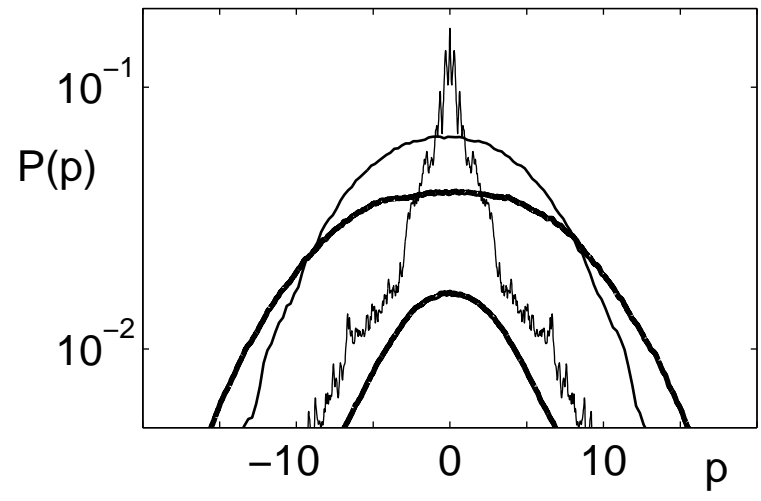
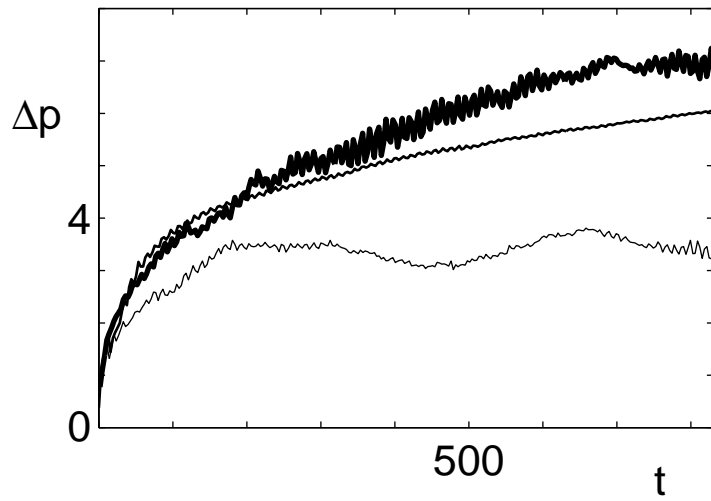
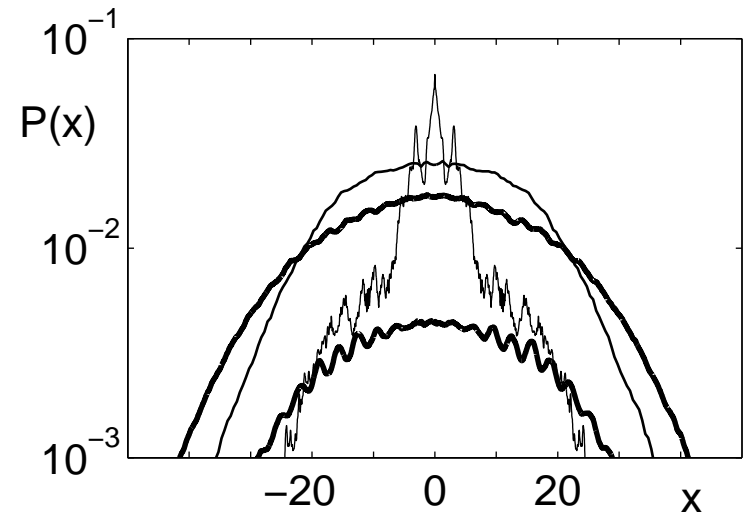
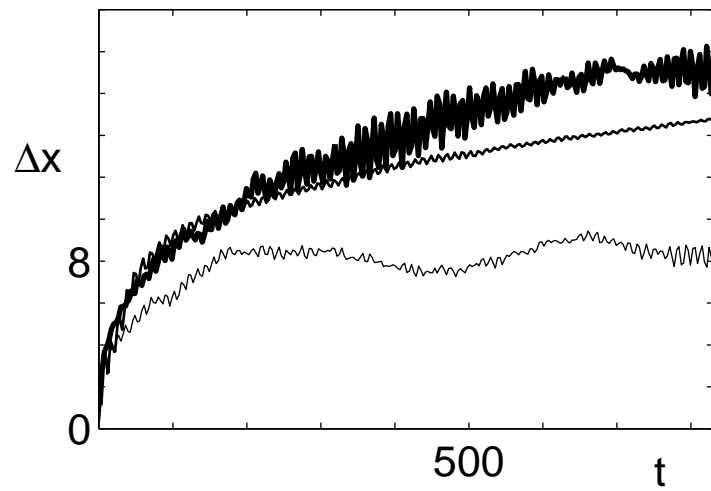


Fig.3, Riedel et al., PRA

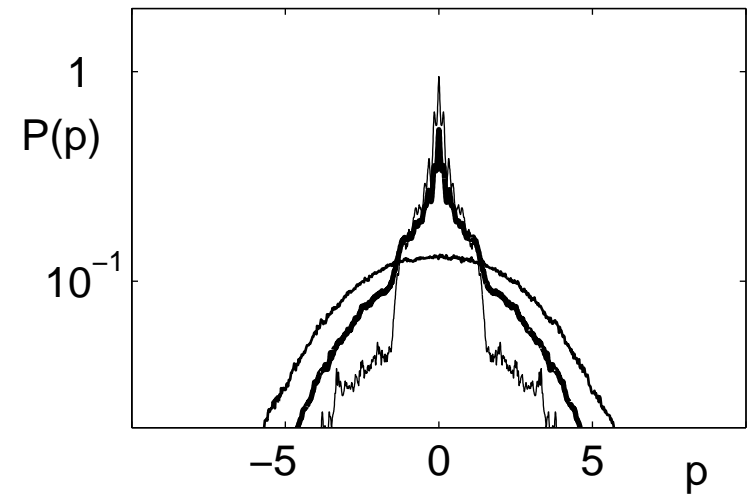
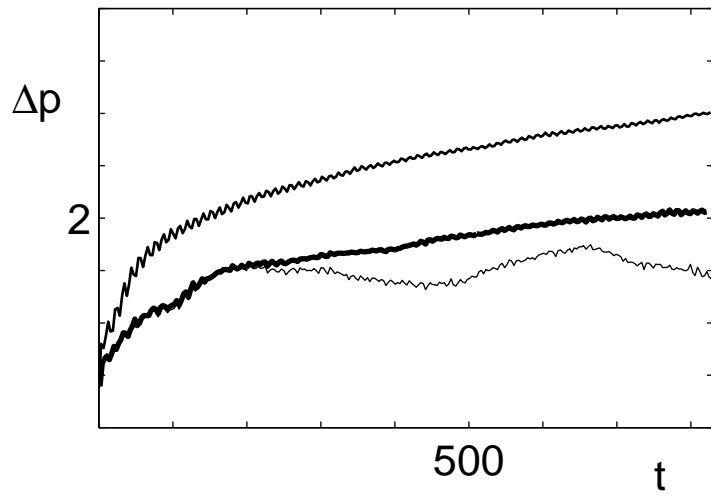
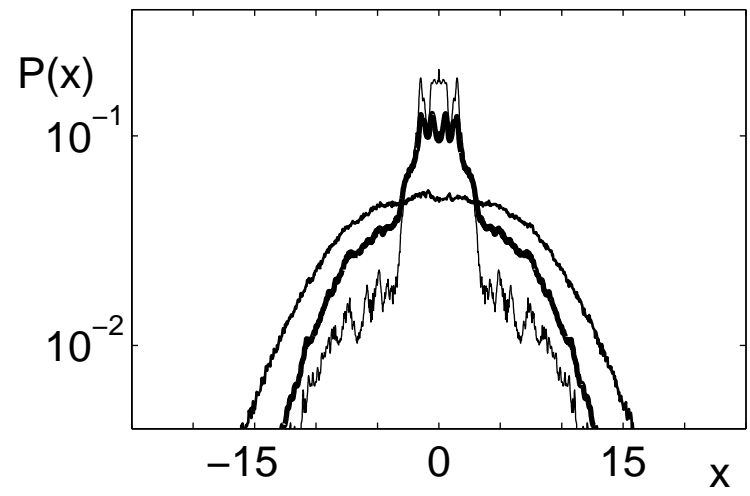
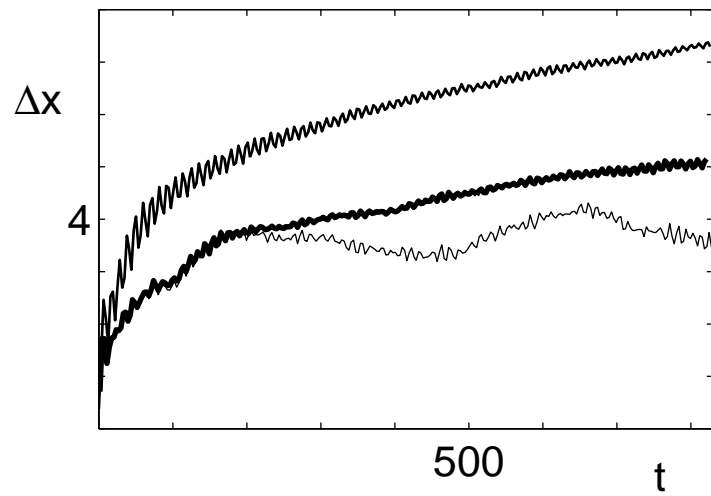


Fig.4, Riedel et al., PRA